CMLS, Cell. Mol. Life Sci. 62 (2005) 1131–1145
1420-682X/05/101131-15
DOI 10.1007/s00018-005-4571-z

CMLS Cellular and Molecular Life Sciences

Research Article

Ethanol inhibits insulin expression and actions in the developing brain

S. M. de la Monte*, X. J. Xu and J. R. Wands

Departments of Pathology and Medicine, Pierre Galletti Research Building, Rhode Island Hospital, 55 Claverick Street, Room 419, Providence, Rhode Island 02903 (USA), Fax: +1 401 444 2939; e-mail: Suzanne_DeLaMonte_MD@Brown.edu

Received 30 December 2004; received after revision 1 March 2005; accepted 10 March 2005

Abstract. Ethanol-induced cerebellar hypoplasia is associated with inhibition of insulin-stimulated survival signaling. The present work explores the mechanisms of impaired insulin signaling in a rat model of fetal alcohol syndrome. Real-time quantitative RT-PCR demonstrated reduced expression of the insulin gene in cerebella of ethanol-exposed pups. Although receptor expression was unaffected, insulin and insulin-like growth factor (IGF-I) receptor tyrosine kinase (RTK) activities were reduced by ethanol exposure, and these abnormalities were associated with increased PTP1b activity. In addition, glucose transporter molecule expression and steady-state levels of ATP were reduced in ethanol-exposed cerebellar tissue. Cultured cerebellar granule neurons from ethanol-exposed pups had reduced expression of genes encoding insulin, IGF-II, and the IGF-I and IGF-II receptors, and impaired insulin- and IGF-I-stimulated glucose uptake and ATP production. The results demonstrate that ethanol inhibits insulin-mediated actions in the developing brain by reducing local insulin production and insulin RTK activation, leading to inhibition of glucose transport and ATP production.

Key words. Ethanol; central nervous system; fetal alcohol syndrome; insulin receptor tyrosine kinase; insulin-like growth factor, type I; protein tyrosine phosphatase

Ethanol exposure during development is one of the leading causes of mental retardation in Europe and North America. Heavy gestational exposure to ethanol can cause fetal alcohol syndrome (FAS), which encompasses a broad array of neurological and systemic lesions including central nervous system (CNS) malformations such as microencephaly, reduced cerebral white matter volume, ventriculomegaly, cerebellar hypoplasia, and disorders of neuronal migration [1]. Experimental models of FAS have demonstrated that the accompanying CNS abnormalities are associated with impaired neuronal survival, growth, synaptogenesis, maturation, neurotransmitter function, and intracellular adhesion [2–7]. However, even shorter durations and lower levels of ethanol exposure can be neurotoxic during development and substantially reduce the populations of CNS neurons [2].

Previous experiments demonstrated that neuronal loss following ethanol exposure was mediated by apoptosis [8-10] or mitochondrial dysfunction [10–13], and subsequent studies correlated these adverse effects of ethanol with inhibition of growth-factor-stimulated survival signaling [9–12]. In the developing CNS, insulin and insulin-like growth factor type 1 (IGF-1) receptors are abundantly expressed [14–16], and the corresponding growth-factor-stimulated responses are critical mediators of neuronal growth, viability, energy metabolism, and synapse formation. Since insulin and IGF-1 signaling pathways are important targets of ethanol toxicity in the immature nervous system [9, 10, 17, 18], neuronal loss

* Corresponding author.

associated with microencephaly in ethanol-exposed fetuses may be caused by ethanol inhibition of insulin/IGF-1-stimulated survival mechanisms.

The stimulatory effects of insulin and IGF-1 are mediated through complex pathways, beginning with ligand binding and activation of intrinsic receptor tyrosine kinases (RTKs) [19, 20], which phosphorylate specific cytosolic molecules, including two of their major substrates, the insulin receptor substrate types 1 (IRS-1) and 2 (IRS-2) [21, 22]. Tyrosyl-phosphorylated IRS-1 (PY-IRS-1) transmits intracellular signals that mediate growth, metabolic functions, and viability by interacting with downstream src homology 2 (SH2)-containing molecules through specific motifs located in the C-terminal region of IRS-1 [21, 22]. The ^{897}YVNI motif of IRS-1 binds to the growth-factor-receptor-bound protein 2 (Grb2) adapter molecule [23, 24]. The ^{1180}YIDL motif binds to Syp protein tyrosine phosphatase, and the 613YMPM and ^{942}YMKM motifs bind to the p85 subunit of phosphatidylinositol-3 kinase (PI3 kinase) [25]. Binding of PY-IRS-1 to p85 stimulates glucose transport [26] and inhibits apoptosis by activating Akt/protein kinase B [27, 28] or inhibiting glycogen synthase kinase-3β (GSK-3β) [29]. Akt kinase inhibits apoptosis by phosphorylating GSK-3β [29, 30] and BAD [31], rendering them inactive. Low levels of Akt kinase and high levels of GSK-3β activity or activated BAD are associated with increased neuronal death [32–34]. BAD inactivates anti-apoptotic Bcl family proteins, rendering the mitochondrial membrane more susceptible to pro-apoptotic molecules that promote membrane permeabilization, cytochrome c release, and caspase activation [35]. Perturbations in mitochondrial membrane permeability increase cellular free radicals that cause mitochondrial DNA damage, mitochondrial dysfunction, and pro-apoptosis cascade activation [36, 37].

Our previous studies showed that ethanol profoundly inhibits insulin-stimulated survival and mitochondrial function in cultured neuronal cells [10, 11], and that chronic gestational exposure to ethanol inhibits insulin-stimulated tyrosine phosphorylation of the insulin receptor and IRS-1, as well as downstream signaling through PI3 kinase and Akt [38, 39]. Impaired insulin-stimulated neuronal survival was found to be associated with increased levels and function of phosphatase and tensin homolog deleted in chromosome 10 (PTEN) [38, 39], which dephosphorylates and negatively regulates PI3 kinase function [40], The present work extends our previous investigations by examining: (i) CNS growth factor production; (ii) insulin and IGF-1 RTK activities; (iii) the activity and expression of protein tyrosine phosphatases that negatively regulate insulin and IGF-1 receptor tyrosine phosphorylation; (iv) glucose transporter gene expression, and (v) growth-factor-stimulated glucose uptake and ATP production. The objective was to characterize potential targets of ethanol neurotoxicity that are likely to contribute to the impaired insulin-stimulated neuronal viability in the developing brain.

Materials and methods

In vivo model of chronic ethanol exposure

Pregnant Long-Evans rats were fed an ethanol-containing (35.4% of the caloric content) or isocaloric control liquid diet (BioServ, Frenchtown, N. J.) beginning on gestation day 6 and continuing throughout pregnancy. Using this protocol, the serum ethanol concentrations in the dams ranged from 35 to 45 mM, which is comparable to the levels observed in human alcoholics [41]. Rats were monitored daily to ensure equivalent caloric consumption and maintenance of body weight. Typically, in the ethanol-fed group, the litter sizes were reduced by 20%, and pup mean body weight was reduced by 10–15%. Studies were conducted with cerebella harvested at birth to evaluate the effects of ethanol in the early postnatal period and prior to the occurrence of any major compensatory developmental responses. Cerebellar tissue was studied because it represents a major in vivo target of ethanol neurotoxicity [2, 42]. Fresh cerebellar tissue was snap frozen in a dry ice-methanol bath and then stored at –80 °C for use in mRNA and protein studies, and assays of kinase or phosphatase activity.

Real-time quantitative RT-PCR assays

For the real-time quantitative RT-PCR studies, total RNA was isolated from cerebellar tissue homogenized in TRIzol reagent (Invitrogen, Carlsbad, Calif.) according to the manufacturer‘s protocol. Prior to use, RNA samples were examined by agarose gel electrophoresis to demonstrate clear bands corresponding to ribosomal RNA and absence of degradation. Samples containing 2 µg RNA were reverse transcribed using the AMV First Strand cDNA synthesis kit (Roche, Basel, Switzerland) and random oligodeoxynucleotide primers. Highly conserved regions of 18S ribosomal RNA and specific mRNAs corresponding to genes of interest were isolated from rat cerebellar tissue by RT-PCR. The complementary (c) DNAs were cloned into the PCRII vector (Invitrogen, Carlsbad, Calif.) and used to generate standard curves for determining transcript abundance (see below). Clone authenticity was demonstrated by DNA sequencing. Control studies included real-time quantitative PCR analysis of: (i) template-free reactions; (ii) RNA that had not been reverse transcribed; (iii) RNA samples that were pre-treated with DNAse I; (iv) samples treated with RNAse A prior to the reverse transcriptase reaction, and (v) genomic DNA.

PCR amplifications were performed using 25-µl reaction volumes containing 20 ng of RT product, 0.4 M each of

Table 1. Primer pairs sequences for real-time quantitative RT-PCR

Primer	Sequence (5′ → 3′)	Position (mRNA)	Amplicon size (bp)
18S	For GGA CAC GGA CAG GAT TGA CA	1278	50
	Rev ACC CAC GGA ATC GAG AAA GA	1327	
Insulin	For TTC TAC ACA CCC AAG TCC CGT C	145	135
	Rev ATC CAC AAT GCC ACG CTT CTG C	279	
Insulin receptor	For TGA CAA TGA GGA ATG TGG GGA C	875	129
	Rev GGG CAA ACT TTC TGA CAA TGA CTG	1003	
IGF-I	For GAC CAA GGG GCT TTT ACT TCA AC	65	127
	Rev TTT GTA GGC TTC AGC GGA GCA C	191	
IGF-I Receptor	For GAA GTC TGC GGT GGT GAT AAA GG	2138	113
	Rev TCT GGG CAC AAA GAT GGA GTT G	2250	
IGF-II	For CCA AGA AGA AAG GAA GGG GAC C	763	95
	Rev GGC GGC TAT TGT TGT TCA CAG C	857	
IGF-II receptor	For TTG CTA TTG ACC TTA GTC CCT TGG	1066	91
	Rev AGA GTG AGA CCT TTG TGT CCC CAC	1156	
IRS-1	For GAT ACC GAT GGC TTC TCA GAC G	604	134
	Rev TCG TTC TCA TAA TAC TCC AGG CG	737	
IRS-2	For CAA CAT TGA CTT TGG TGA AGG GG	255	109
	Rev TGA AGC AGG ACT ACT GGC TGA GAG	363	
IRS-4	For ACC TGA AGA TAA GGG GTC GTC TGC	2409	132
	Rev TGT GTG GGG TTT AGT GGT CTG G	2540	
GLUT-1	For CGC TTC CTG CTC ATC AAT CG	842	115
	Rev GCC GAC CCT CTT CTT TCA TCT C	956	
GLUT-2	For TGT TTT GGG TGT TCC TCT GGA TG	240	100
	Rev TGG TGT CGT ATG TGC TGG TGT G	339	
GLUT-3	For AAG AGC GGT TGG AAG ACC TAC C	224	126
	Rev CAA AGC GGT TGA CAA AGA GTC C	349	
GLUT-4	For TTG GGT TTG GAG TCT ATG CTG G	753	109
	Rev TCT CAG GAC AGA AGG GCA ACA G	861	
PTP-S	For CAG AGG CTA AAT GAA ACT GAA CGG	1060	183
	Rev CAA CTT GTG AGG CAA TCT ACA GGG	1242	
PTP-1	For CAA CCG AGG AGG AAC AAA AGG	1297	129
	Rev CAG TCT GTC AGT GAA AAC ATA CCC G	1425	
PP1	For CGG CGA GTT TGA CAA TGC TG	1080	257
	Rev TGG CTG GAT GGT TTT ACA GTG C	1336	
PP2A	For CAG TAA AGG GAC CAT TCG CTT ATG	1022	106
	Rev AAA AAA CGA CCT GTT GCT GGG	1127	

IGF-I, insulin-like growth factor type I; IGF-II, insulin-like growth factor type II; IRS, insulin receptor substrate; GLUT, glucose transporter; PTP-S, protein tyrosine phosphatase, non-receptor type 2; PTP-1, protein tyrosine phosphatase, non-receptor type 1; PP1, protein phosphatase 1; PP2, protein phosphatase 2.

the forward and reverse primers (table 1), and SYBR Green I PCR reagent (Qiagen, Valencia, Calif.). The amplified signals were detected continuously with the Bio-Rad iCycler and the iQ Multi-Color Real Time PCR Detection System (Hercules, Calif.). The following real-time PCR amplification protocol was used: (i) initial denaturation at 95 °C for 10 min; (ii) a 3-segment amplification and quantification program consisting of 40 cycles of 95 °C for 15 s, 55–65 °C for 45 s, and 72 °C for 30 s; and (iii) a sustained cooling step down to 4 °C. Annealing temperatures were optimized using the iCycler temperature gradient program. In preliminary studies, SYBR Green-labeled PCR products were evaluated by agarose gel electrophoresis, and the authenticity of each amplicon was verified by nucleic acid sequencing. In addition, immediately after the amplifications, the iCycler Melt Curve program was run to verify the presence of a single peak and absence of primer-dimers in each template-containing reaction.

The data obtained by real-time quantitative RT-PCR were used to calculate relative expression level of each mRNA transcript examined. To accomplish this, serial dilutions of known quantities of purified recombinant plasmid DNA containing the specific target sequences were used as standards in the PCR reactions, and the equations of the regression lines relating cycle threshold (C_t values) to

nanograms of DNA were used to calculate mRNA transcript abundance in the samples. To correct for small differences in template loading, the nanograms ratios of specific mRNA to 18S were calculated, thereby providing normalized indices of relative transcript abundance that were used to make inter-group comparisons [38]. The 18S RNA content was used as the denominator because the levels were highly abundant and essentially invariant, whereas housekeeping genes were modulated with disease state. Between-group statistical comparisons were made using the calculated mRNA/18S ratios.

Western blot analysis and immunoprecipitation studies

For Western blot analysis, rat pup cerebella were individually Polytron homogenized in radio-immunoprecipitation assay (RIPA) buffer (50 mM Tris-HCl, pH 7.5, 1% NP-40, 0.25% sodium deoxycholate, 150 mM NaCl, 1 mM EDTA, 2 mM EGTA) containing protease and phosphatase inhibitors (1 mM NaF, 1 mM $Na_4P_2O_7$, 2 mM Na3VO4, 1 mM phenylmethylsulfonyl fluoride, 1 µg/ml each of aprotinin, pepstatin A, and leupeptin) [43]. For immunoprecipitation, homogenates were prepared in Triton lysis buffer (50 mM Tris-HCI, pH 7.5, 10 mM EDTA, 1% Triton X-100) containing protease and phosphatase inhibitors as indicated. Cellular debris was pelleted by centrifuging the samples at 14,000 g for 15 min at 4 °C, and the resulting supernatant fractions were used in the studies. Protein concentration was measured with the Bicinchoninic Acid (BCA) assay (Pierce, Rockford, Ill.). Aliquots containing 60 µg protein were used for Western blot analysis [17, 44, 45], and 100- or 250-µg samples were used for immunoprecipitation/Western immunoblotting or kinase assays [11, 17]. Immunoreactivity was detected with horseradish-peroxidase-conjugated secondary antibody and SuperSignal enhanced chemiluminescence reagents (Pierce). Immunoreactivity was revealed and quantified using the Kodak Digital Science Imaging Station (DuPont-NEN Life Sciences Products, Boston, Mass.).

RTK assays

Insulin or IGF-I receptor molecules were immunoprecipitated from individual 100-µg protein samples using rabbit polyclonal antibodies (1 µg/ml) and protein A sepharose (Amersham-Pharmacia, Arlington Heights, Ill.) [43]. RTK activity was measured in the immune precipitates using a non-isotopic assay (Chemicon International, Temecula, Calif.) according to the manufacturer's protocol with small modifications. Briefly, tyrosine phosphorylation of the biotinylated synthetic peptide substrate captured onto streptavidin-coated wells was detected with horseradish-peroxidase-conjugated anti-phosphotyrosine and SuperSignal West Pico Chemiluminescent substrate (Pierce). Luminescence was measured in a TopCount machine (Packard Instrument Co., Meriden, Conn.). The immunoprecipitants captured onto protein A were subjected to Western blotting with densitometry to normalize the levels of tyrosine kinase activity to the receptor protein content in the reactions.

Assays of phosphatase gene expression and phosphatase activity

RNA was reverse transcribed using random primers, and mRNA transcripts corresponding to protein tyrosine phosphatase, type 1 (PTP-1b), protein tyrosine phosphatase, type 2 (TCPTP/PTP-S), protein phosphatase 1 (PP1), and protein phosphatase 2 (PP2) were measured by real-time quantitative RT-PCR using gene-specific primers (table 1). The nanogram quantities of mRNA were normalized to 18S ribosomal RNA measured in the same samples. PTP1b/PTP-S, PP1, and PP2A activities were measured using specific peptide substrates and a malachite-green-based assay. PTP1b and PTP-S utilize the same substrate, and therefore their activities could not be distinguished. Briefly, fresh frozen cerebellar tissue was Polytron (Glen Mills, Clifton, N. J.) homogenized in 5 vol buffer containing 40 mM Tris-HCl, pH 7.4, 2 mM EDTA, 50 mM NaF, 1% NP-40, 1 mM $Na_4P_2O_7$, and protease inhibitors as indicated above. The samples were centrifuged at 14,000 g for 15 min at 4 °C, and the supernatants were used directly in the phosphatase assays. Protein concentrations were determined using the BCA assay. Assays of PTP-1b/PTP-S activity were performed in 50-µl reactions containing 150 M synthetic peptide substrate (Asp Ala Asp Glu pTyr Leu Ile Pro Gln Gln Gly) (Biomol Research Laboratories, Plymouth Meeting, Pa.), 25 mM HEPES, pH 7.2, 1 mM DTT, 1 mM EDTA, and 0.1% NP-40. The dephosphorylation reactions were initiated by adding cerebellar protein extract (10 g). Replicate assays were performed in the presence of a Ser/Thr phosphatase inhibitor cocktail to verify specificity of the results.

PP2A activity was assayed in 50-µl reactions containing 100 µM threonine phosphopeptide (Lys Arg pThr Ile Arg Arg) (Upstate Biotechnology, Grand Island, N. Y.), 50 mM Tris-HCl, pH 7.5, 1 mM DTT, and 0.1 mM EGTA. PHI-1 (1 M; Upstate, Charlottesville, Va.) was added to inhibit PP1 activity. PP1 activity was measured under the same conditions, but in the presence of 2 nM okadaic acid (Calbiochem, Carlsbad, Calif.), which inhibits PP2A. The dephosphorylation reactions were initiated by adding 500 µg cerebellar protein homogenate. All phosphatase assay incubations were carried out at 22 °C for 30 min and terminated by adding 100 l Biomol Green reagent (Biomol Research Laboratories, Pa.). Absorbances were measured at 620 nm using a SpectraCount machine (Packard Instrument Co.). Phosphate release was determined from a standard curve relating OD_{620nm} to nmol PO_4. The experimental data were expressed as nmol phosphate released/µg protein.

Analysis of gene expression in cerebellar granule neuron cultures

In vitro experiments were used to examine gene expression in cerebellar neurons isolated from control and ethanol-exposed pups. These studies were used to determine the degree to which ethanol-associated alterations in gene expression occurred in neurons, as opposed to other cell types present in the tissue homogenates. Primary neuronal cultures were generated with cerebellar tissue harvested from postnatal day 1 control and ethanol-exposed pups [46]. Fluorescence-activated cell sorting demonstrated that greater than 95% of cells isolated from control and ethanol-exposed pup cerebella were neuronal as evidenced by immunoreactivity with antibodies to HuC/HuD neuron-specific RNA-binding protein [47] (Molecular Probes, Eugene, Ore.) (data not shown). Cultures were maintained for 2 days in Dulbecco's modified Eagle's medium (DMEM) supplemented with 5% fetal calf serum, 4 mM glutamine, 10 mM non-essential amino acid mixture (Gibco-BRL, Grand Island, N. Y.), 25 mM KCl, and 9 g/l glucose, after which the cells were harvested for quantitative real-time RT-PCR analysis of gene expression.

Cell culture models for examining the effects of short-term ethanol on insulin/IGF-1 stimulated neuronal gene expression and function

To investigate the direct effects of ethanol on insulin-stimulated functions, primary cerebellar granule neuron cultures were seeded into 12- or 24-well plates. After 5 days in culture, the cells were treated with 6 µM cytosine arabinoside to inhibit DNA synthesis. The cultures were then exposed to 50 mM ethanol or nothing for 2 days using sealed humidified chambers [17, 44], after which they were serum-starved for 12 h, then stimulated with 50 nM insulin or 25 nM IGF-1 in the presence or absence of 50 mM ethanol. The studies were focused on examining the effects of ethanol on insulin- and IGF-1-stimulated glucose uptake. Parallel 96-well microcultures in which 5×10^4 viable cells (determined by Trypan Blue exclusion) were seeded per well were used to measure insulin- and IGF-I-stimulated ATP using the ATPLite assay (Packard Instrument Co.).

Glucose uptake assay

Primary cerebellar neuron cultures seeded in 12-well plates were treated with nothing or 50 mM ethanol for 2 days in sealed chambers [48, 49], after which they were serum-starved overnight. The cells were then washed with serum-free medium and incubated with pre-warmed depletion medium [DMEM containing 4 mM glutamine, 25 mM KCl, and 9 g/l glucose, 0.5% bovine serum albumin (BSA), and 25 mM HEPES] for 3 h at 37 °C. After rinsing once in glucose-free DMEM, the cultures were incubated for 20 min at 37 °C with glucose-free DMEM supplemented with no growth factor, 50 nM insulin or 25 nM IGF-I, after which they were transferred to a 37 °C shaking water bath and incubated for 10 min further with 50 µM 2-deoxyglucose, 0.5 µCi/ml ^{3}H-2-deoxyglucose ± 25 µM cytochalasin B or vehicle [50–52]. The cultures were chilled on ice, and after three rinses with ice-cold PBS, the cells were lysed with 500 µl/well 0.1% Triton X-100 in PBS. To measure ^{3}H 2-deoxyglucose uptake, 450 µl of each lysate was transferred to vials containing 4.5 ml of aqueous scintillation fluid, and the samples were counted in a Beckman Scintillation Counter. The remaining 50 µl of sample was used to measure protein concentration using the BCA assay. Glucose uptake levels were normalized to protein concentration and expressed as pmol/mg protein per minute.

ATP assays

ATP levels were measured directly in cultured cells or in snap-frozen cerebellar homogenates using the ATPLite assay system (Perkin-Elmer, Boston, Mass.). Cultured cells were lysed by replacing the medium with 100 µl H_2O and adding 50 µl of ATP lysis solution (provided with the kit). The lysates were serially diluted and 50 µl ATP substrate was added per 150 µl lysate. Snap-frozen cerebellar tissue samples were Polytron homogenized in three volumes of PBS containing 20 mM glycine, 50 mM $MgSO_4$, and 4 mM EDTA. Aliquots 100 µl were transferred to 96-well black plates and serially diluted in water, maintaining final volumes of 100 µl per well. ATPLite lysis buffer (50 µm) was added to each diluted sample. The plates were covered with adhesive plastic sheets and agitated at 700 rpm for 5 min at room temperature. Then, 50 µl of ATPLite substrate was added to each sample, and the sealed plates covered with aluminum foil were agitated for an additional 5 min (700 rpm at room temperature). Luminescence was measured in a TopCount machine (Packard Instrument Co), and ATP relative light unit values were normalized to protein concentration.

Source of reagents

Polyclonal antibodies to the insulin or IGF-I receptor were purchased from Santa Cruz (Santa Cruz, Calif.). Insulin (humulin) was purchased from Eli Lilly & Co. (Indianapolis, Ind.). Recombinant IGF-I, 2-deoxyglucose and cytochalasin B were purchased from Sigma-Aldrich, (St. Louis, Mo.). ^{3}H-2-deoxyglucose was purchased from New England Nuclear (Boston, Mass.). All other reagents were purchased from Calbiochem or Sigma-Aldrich. GLUT4 rabbit polyclonal antibody was generously provided by Dr. R. Bradley (Joslin Diabetes Center, Boston, Mass.).

Statistical analysis

Inter-group comparisons were made with the Student t test or analysis of variance and the Fisher least signifi-

cance post hoc significance test using the Number Cruncher Statistical System (Dr. J. L. Hintze, Kaysville, Utah).

Results

General comments regarding quantitative RT-PCR studies

The use of real-time quantitative RT-PCR enabled all samples to be analyzed simultaneously and with sufficient replicates to demonstrate consistency of results. With the techniques employed, the quality of the cDNA templates generated from brain tissue was judged to be excellent based on the similar 18S C_t values and consistent 28S:18S ratios obtained for both the control and ethanol-exposed brains. In addition, the 28S:18S ratios were uniformly comparable to the values obtained for RNA isolated from primary neuronal cultures or cell lines. Typically, with cDNA prepared from 10 ng of total RNA, the 18S Ct values ranged from 8 to 10, and the calculated 28S:18S ng ratios ranged from 2.0 to 2.2 as previously reported for brain tissue using Northern blot or slot blot analysis [53, 54]. The use of real-time quantitative RT-PCR was ideally suited for rigorous analysis of gene expression in brain tissue because the amplicons were small (mainly <150 bp), thereby circumventing any potential problems related to partial RNA degradation, e.g. nicking, which may increase with oxidative stress or sample processing. The specificity of the amplified products was verified by direct nucleic acid sequencing. Control studies in which cDNA templates were excluded, RNA was not reverse transcribed, the RNA samples were pre-treated with RNAse A prior to the RT step, or genomic DNA was used in the reactions had no detectable amplified products by real-time PCR analysis and agarose gel electrophoresis. Treatment of the RNA samples with DNAse I prior to the RT step had no effect on the detection levels of amplified gene products.

Effects of chronic gestational exposure to ethanol on growth factor receptor, growth factor, and insulin receptor substrate gene expression in cerebellar tissue

Real-time quantitative RT-PCR studies detected mRNA transcripts corresponding to genes for insulin, IGF-I, and IGF-II receptors, insulin, IGF-I, and IGF-II polypeptides, and IRS-1, IRS-2, and IRS-4 in both control and ethanol-exposed cerebella (fig. 1). The nanogram quantities of each specific mRNA transcript detected were normalized to the 18S RNA levels measured in the same samples, and results from 8 to 12 animals per group were analyzed statistically. In control cerebella, insulin and IGF-I receptor mRNA levels were similar, and 15- to 20-fold higher than the levels of IGF-II receptor (figs. 1A–C). Chronic gestational exposure to ethanol had no significant effect on the levels of insulin or IGF-I receptor expression, but it was associated with significantly increased levels of IGF-II receptor expression (figs. 1A–C). Among the growth factors, IGF-II mRNA transcripts were most abundant, followed by IGF-I, and then insulin (figs. 1D–F). Chronic gestational exposure to ethanol resulted in significantly reduced levels of insulin polypeptide gene expression (fig. 1D), and significantly increased levels of IGF-II gene expression (fig. 1F), but no significant alteration in IGF-I expression (fig. 1E). Among the IRS genes, in control brains, IRS-2 and IRS-4 mRNA transcripts were similarly abundant, and both were three- to four-fold higher than IRS-1. In the ethanol-exposed group, IRS-4 expression was relatively reduced and similar to IRS-1, whereas IRS-2 expression was four- to five-fold higher than IRS-1 or IRS-4. There were no statistically significant differences observed with respect to the mean levels of the IRS transcripts measured in control and ethanol-exposed cerebella (figs. 1G–H).

Effects of chronic gestational exposure to ethanol on growth factor receptor, growth factor polypeptide, and insulin receptor substrate gene expression in isolated cerebellar granule neurons

To examine the effects of gestational exposure to ethanol on gene expression in isolated neuronal cells, short-term (2 days) primary cultures were generated from cerebella of control and ethanol-exposed pups. The real-time quantitative RT-PCR studies demonstrated some differences in the relative mRNA levels of growth factor receptor, growth factor, and IRS gene expression between the cerebellar tissue samples and the corresponding neuronal cultures generated from cerebella (fig. 2). In control samples, insulin receptor expression was approximately threefold lower in the cultures, whereas IGF-I receptor expression was similar, and IGF-II receptor expression was slightly increased (twofold). With regard to the growth factors, insulin gene expression was approximately tenfold lower, and IGF-I expression was nearly 100-fold lower in the cultures compared with the tissue samples. In contrast, IGF-II gene expression was slightly higher (threefold) in the cultured neurons. IRS-1 expression was nearly fourfold higher and IRS-4 expression was approximately threefold lower in the cultured control neurons compared with control cerebellar tissue. In contrast, IRS-2 expression was similar in the neuronal cultures and cerebellar tissues.

The real-time quantitative RT-PCR studies demonstrated that in control neurons, IGF-I receptor expression was most abundant, followed by insulin receptor, and then IGF-II receptor, whereas in the ethanol-exposed neurons, IGF-I and insulin receptors were similarly abundant, and both were more highly expressed (five- to sixfold) than IGF-II receptors. Inter-group comparisons demonstrated that

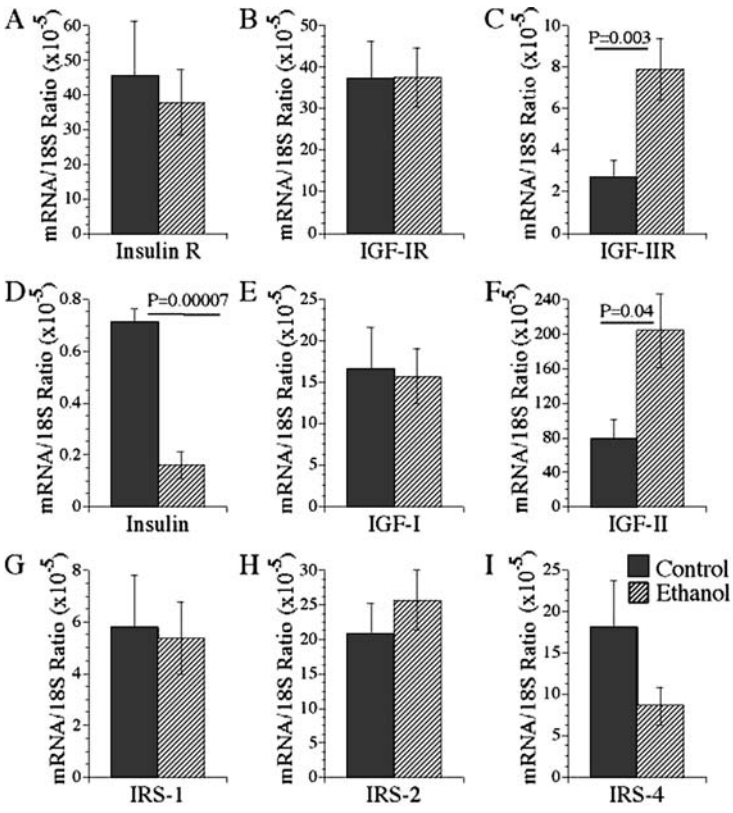

Figure 1. Effects of chronic gestational exposure to ethanol on cerebellar expression of insulin receptor (R) (*A*), IGF-IR (*B*), IGF-IIR (*C*), insulin (*D*), IGF-I (*E*), IGF-II (*F*) polypeptide genes, and IRS-1 (*G*), IRS-2 (*H*), and IRS-4 (*I*) in an in vivo model of FAS. RNA was extracted from postnatal day 1 rat pup cerebellar tissue and reverse transcribed using random primers. The mRNA transcripts were measured using gene-specific primers (table 1) and real-time quantitative RT-PCR. The nanogram quantities of mRNA were normalized to 18S ribosomal RNA measured in the same samples. Graphs depict the mean ± SE of results. Data were analyzed statistically using Student t tests. Significant p values (including trends) are indicated over the bar graphs. Solid bars, control; hatched bars, ethanol exposed.

ethanol-exposed neuronal cells had significantly reduced levels of both IGF-I and IGF-II receptors, but similar levels of insulin receptor relative to control neurons (figs. 2A–C). With regard to the growth factors, in both control and ethanol-exposed neurons, IGF-II was more abundantly expressed than IGF-I, which was more abundant than insulin (figs. 2D–F). The ethanol-exposed neuronal cultures had significantly reduced mean levels of insulin and IGF-II gene expression, but no significant alteration in the mean level of IGF-I expression (figs. 2D–F). Corresponding with the results obtained using cerebellar tissue, no significant inter-group differences were observed with respect to the levels of IRS-1, IRS-2, or IRS-4 in the control and ethanol-exposed cerebellar neurons (figs 2G–I).

Effects of gestational ethanol exposure on insulin and IGF-I RTK activities

Although there were no significant differences in the mRNA levels of insulin and IGF-I receptors in control and ethanol-exposed cerebella, and the levels of insulin receptor gene expression were similar in control and ethanol-exposed cerebellar neurons, previous studies demonstrated that ethanol treatment inhibits growth-factor-stimulated insulin receptor tyrosine phosphorylation [38]. Therefore, further studies were done to determine if chronic ethanol exposure constitutively inhibits insulin and IGF-I RTK activities. RTK activities were measured in immunoprecipitates using a non-isotopic luminescence-based detection assay. The studies demonstrated significantly reduced levels of both insulin- and IGF-I RTK activities in cerebella from ethanol-exposed relative to control pups (figs. 3A, B). Since the results were normalized to insulin and IGF-I receptor protein levels in the immunoprecipitates (as detected by Western blot analysis with densitometry), the reduced levels of tyrosine kinase activity measured in the ethanol-exposed samples were not attributable to ethanol inhibition of growth factor receptor expression.

Ethanol inhibition of receptor tyrosine kinase activity is associated with increased protein tyrosine phosphatase activity

Since insulin and IGF-I receptor expression were not significantly reduced in the ethanol-exposed cerebellar tis-

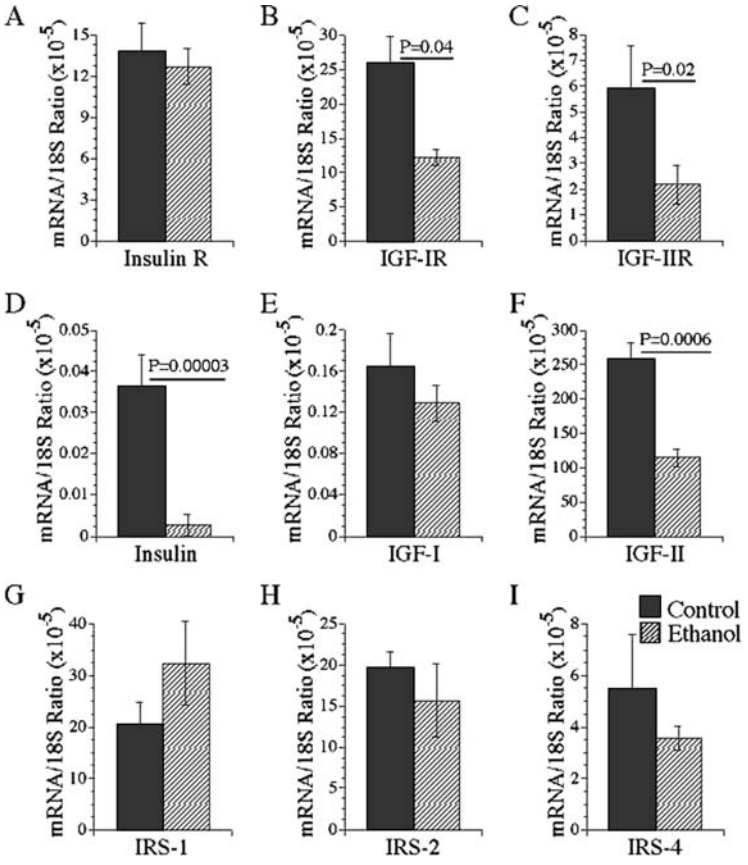

Figure 2. Expression of insulin receptor (R) (*A*), IGF-IR (*B*), IGF-IIR (*C*), insulin (*D*), IGF-I (*E*), IGF-II (*F*) polypeptide genes, and IRS-1 (*G*), IRS-2 (*H*), and IRS-4 (*I*) in primary neuronal cultures generated from the cerebella of control and ethanol-exposed postnatal day 1 pups. RNA was reverse transcribed using random primers, and mRNA transcripts were measured using gene-specific primers (table 1) and real-time quantitative RT-PCR. The nanogram quantities of mRNA were normalized to 18S ribosomal RNA measured in the same samples. Graphs depict the mean ± SE of results. Data were analyzed statistically using Student t tests. Significant p values (including trends) are indicated over the bar graphs. Solid bars, control; hatched bars, ethanol exposed.

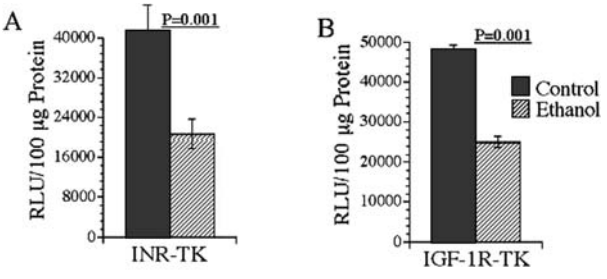

Figure 3. Measurement of insulin receptor (INR-TK) (*A*) and IGF-I receptor (IGF-1R-TK) (*B*) tyrosine kinase activities in control and ethanol-exposed cerebellar tissue isolated from postnatal day 1 rat pups. Insulin or IGF-I receptor immunoprecipitates (from 100 µg protein homogenates) were analyzed for tyrosine kinase activity using biotinylated synthetic peptide substrates that were captured onto streptavidin-coated surfaces. Tyrosine phosphorylation of the substrates was detected with horseradish-peroxidase-conjugated anti-phosphotyrosine and enhanced luminescence reagents. Luminescence relative light units (RLU) were measured in a TopCount machine. The results were normalized to receptor protein expression detected by Western blot analysis of the immune precipitates. Data were analyzed statistically using Student t tests. Significant p values are indicated over the bar graphs. Solid bars, control; hatched bars, ethanol exposed.

sues, the mechanism by which insulin and IGF-I RTK activities were reduced by ethanol were likely functional in nature. Previous studies demonstrated that ethanol inhibition of insulin signaling downstream through PI3 kinase-Akt was mediated by increased expression and activation of PTEN phosphatase [38, 39]. Therefore, further studies were performed to determine if increased phosphatase gene expression or activity could account for reduced signaling through the insulin and IGF-I receptors. PTP1b and PTP-S/TCPTP negatively regulate insulin sensitivity by dephosphorylating the insulin or IGF-I receptor [55, 56], and could account for ethanol-associated reductions in the corresponding RTK activities. PP1 and PP2A were also studied because of their broad roles in regulating cell growth. Real-time quantitative RT-PCR assays demonstrated no significant differences between the control and ethanol-exposed cerebellar tissue samples with respect to the mRNA levels of PP1, PP2A, PTP-1b, and PTP-S/TCPTP (figs. 4A–D). However, enzymatic studies demonstrated slightly higher but not significantly differ-

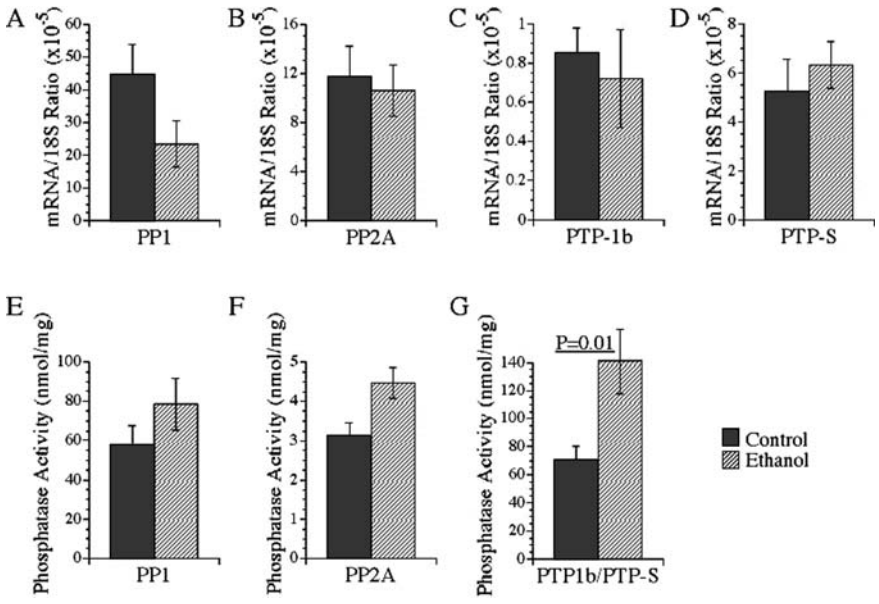

Figure 4. Effects of chronic gestational exposure to ethanol on phosphatase gene expression (*A–D*) and phosphatase activity (*E–G*) in the brain. RNA was extracted from postnatal day 1 rat pup cerebellar tissue, reverse transcribed using random primers, and mRNA transcripts corresponding to PP1 (*A*), PP2A (*B*), PTP-1b (*C*), and PTP-S/TCPTP (*D*) were measured by real-time quantitative RT-PCR using gene specific primers (table 1). The nanogram quantities of mRNA were normalized to 18S ribosomal RNA measured in the same samples. PP1 (*E*), PP2A (*F*), and PTP1b/PTP-S (*G*) activities were measured in cerebellar protein extracts using specific synthetic peptide substrates and a malachite-green-based assay (see Material and methods). PTP1b and PTP-S utilize the same substrate and cannot be distinguished with the methods employed. Data were analyzed statistically using Student t tests. Significant p values are indicated over the bar graphs. Solid bars, control; hatched bars, ethanol exposed.

ent levels of PP1 and PP2A activities in the ethanol-exposed group relative to control groups (figs. 4E, F), and significantly increased levels of PTP1b/PTP-S activity in the ethanol-exposed relative to control cerebella (fig. 4G). PTP1b and PTP-S activities were measured together because these enzymes utilize the same substrate.

Gestational exposure to ethanol inhibits glucose transporter gene expression and ATP production in the brain

Since we observed reduced local growth factor production and impaired RTK activities, further studies were conducted to characterize the effects of ethanol on glucose transporter molecule expression, glucose uptake, and ATP production. Using real-time quantitative RT-PCR, GLUT1, GLUT2, GLUT3, and GLUT4 mRNA transcripts were found to be similarly abundant in control cerebella, i.e., there was no differential pattern of GLUT gene expression in normal early postnatal cerebellar tissue (figs. 5A–D). In contrast, chronic gestational exposure to ethanol resulted in significantly reduced levels of GLUT2 and GLUT4, significantly increased levels of GLUT1, and unaltered GLUT3 mRNA expression (figs. 5A–D). Western blot analysis with densitometry further demonstrated that the significantly reduced mean level of GLUT4 mRNA was associated with a correspondingly reduced mean level of GLUT4 protein in the ethanol-exposed group (fig. 5E). In contrast, β-actin expression levels were similar in the control and ethanol-exposed samples (data not shown). ATP levels were measured in cerebellar homogenates using a luminescence-based assay (ATPLite). The studies demonstrated significantly reduced (fivefold) levels of ATP in ethanol-exposed relative to control cerebellar tissue (fig. 5F).

Ethanol inhibits glucose uptake and ATP production in neuronal cells

To determine the effects of ethanol on glucose uptake and ATP production, control and ethanol-exposed cerebellar granule neuron cultures were serum starved for 12 h, then stimulated with 50 nM insulin, 25 nM IGF-I, or nothing (vehicle) for 2 h. Glucose uptake was measured using a ^{3}H-deoxyglucose assay, and ATP levels were measured using the ATPLite assay. Control cells had mean glucose uptake values of ~34 pmol/mg per minute, and slightly higher uptake levels following insulin (44 pmol/mg per minute) or IGF-I (~38 pmol/mg per minute) stimulation. Neuronal cultures generated from ethanol-exposed cerebella had significantly reduced basal and insulin- or IGF-I stimulated levels of glucose uptake relative to corresponding control cultures (fig. 6A). In control cerebellar neuron cultures, the basal levels of ATP were relatively high, and ATP production was increased more effectively by IGF-1 than insulin stimulation (fig. 6B). In the

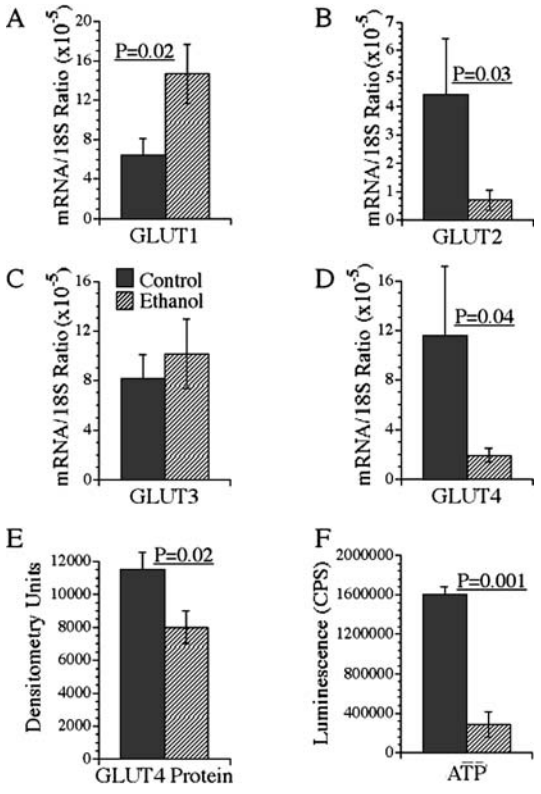

Figure 5. Effects of chronic gestational exposure to ethanol on glucose transporter (GLUT) gene expression and ATP levels in cerebellar tissue. RNA extracted from postnatal day 1 rat pup cerebella was reverse transcribed using random primers, and mRNA transcripts corresponding to GLUT1 (*A*), GLUT2 (*B*), GLUT3 (*C*), and GLUT4 (*D*) were measured by real-time quantitative RT-PCR using gene-specific primers (table 1). The nanogram quantities of mRNA were normalized to 18S ribosomal RNA measured in the same samples. GLUT4 protein levels were measured by Western blot analysis and with densitometric quantification (*E*). ATP levels were measured in cerebellar homogenates using the ATPLite luminescence assay (*F*). Luminescence counts per second (CPS) were measured in a TopCount machine. Data were analyzed statistically using Student t tests. Significant p values are indicated over the bar graphs. Solid bars, control; hatched bars, ethanol exposed.

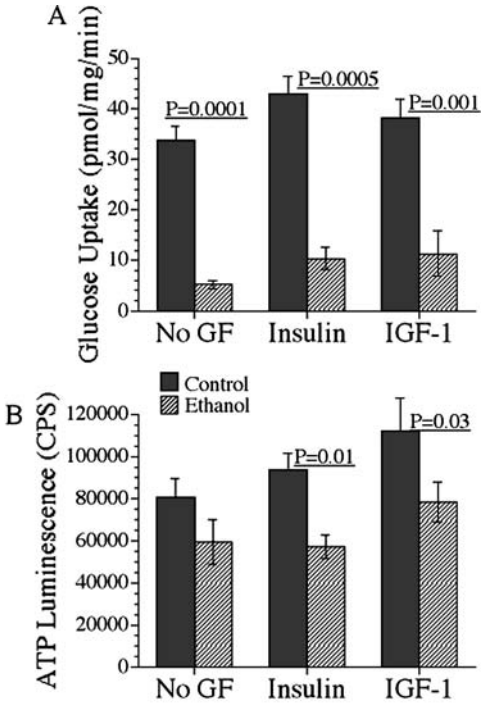

Figure 6. Short-term ethanol exposure inhibits glucose uptake and ATP production in CNS neurons. Primary neuronal cultures were generated from control (normal) cerebella of postnatal day 1 pups. After 5 days in culture, the cells were exposed to 50 mM ethanol or nothing for 48 h in sealed chambers that were equilibrated with humidified air (74% nitrogen, 21% oxygen, 5% CO_2). Ethanol was added to the reservoir tray to allow for vaporization. The cells were serum starved overnight, then stimulated with nothing (basal conditions), 50 nM insulin, or 25 nM IGF-I for 30 min. Glucose uptake (*A*) was measured using ^{3}H-2-deoxyglucose (see Material and methods), and ATP levels (*B*) were measured using the ATPLite luminescence assay. Luminescence counts per second (CPS) were measured in a TopCount machine. Data were analyzed statistically using ANOVA and the Fisher post hoc test. Significant p values are indicated over the bar graphs. Solid bars, control; hatched bars, ethanol exposed.

ethanol-exposed cultures, ATP levels were consistently lower than in the control, and growth factor stimulation resulted in either no detectable or only modestly increased ATP production, resulting in levels that were still significantly lower than control (fig. 6B).

Discussion

Effects of chronic gestational exposure to ethanol on in vivo expression of genes required for insulin and IGF signaling

In previous studies, we demonstrated that chronic gestational exposure to ethanol results in cerebellar hypoplasia with neuronal loss due to increased apoptosis [38]. Those mutagenic effects of ethanol were accompanied by reduced levels of tyrosine-phosphorylated insulin receptor, tyrosine-phosphorylated IRS-1, and p85 associated IRS-1, i.e., IRS-1-associated PI3 kinase activity [38]. The current studies focused on characterizing the mechanisms and functional consequences of impaired insulin signaling, and explored some of the effects of ethanol on IGF-I and IGF-II signaling pathways. Corresponding with the results of previous investigations using Western blot analysis, insulin receptor mRNA expression was found to be similar in the control and ethanol-exposed cerebellar tissue as demonstrated by real-time quantitative RT-PCR. Similarly, IGF-I receptor gene expression levels in cerebellar tissue were not reduced by chronic gestational exposure to ethanol. In contrast, IGF-II receptor expression was significantly increased in the ethanol-exposed cerebella, perhaps reflecting a compensatory response to impaired insulin signaling, or a shift in the resultant cell population following neurotoxic death of cerebellar neurons.

The experimental approach of transiently culturing isolated cerebellar granule neurons enabled us to determine the effects of chronic gestational exposure to ethanol on gene expression in neuronal cells and minimize contributions from other structures and cell types since greater than 95% of the isolated cells were characterized as Hu^+ neurons. The in vitro experiments demonstrated significantly reduced levels of IGF-I and IGF-II receptor expression in neuronal cells isolated from ethanol-exposed brains. This suggests that the IGF-I- and IGF-II-receptor-bearing neurons may represent vulnerable targets of ethanol neurotoxicity. Moreover, the similar levels of IGF-I and IGF-II receptors detected in brain tissue may reflect increased expression of these genes in non-neuronal cells such as glial and vascular cells. The lower levels of insulin receptor gene expression detected in vitro compared with in vivo suggest that insulin receptors are more abundantly expressed in non-neuronal compared with neuronal cells in the early postnatal cerebellum. Future studies will determine if the ethanol-associated reductions in neuronal IGF-I and IGF-II receptor transcripts reflect down-regulation of those genes, or progressive loss of cells with these phenotypes.

The real-time quantitative RT-PCR studies demonstrated expression of insulin, IGF-I, and IGF-II polypeptide mRNA transcripts in cerebellar tissue, and the analysis of neuronal cultures established that CNS neurons express mRNA transcripts corresponding to each of these growth factors. Although previous studies demonstrated IGF-I and IGF-II expression in the brain [57, 58], whether neuronal cells could express the insulin polypeptide gene remained questionable until now. The major obstacle was in determining if the insulin immunoreactivity reflected transport of insulin from the blood or endogenously produced molecules in the CNS. The detection of insulin polypeptide mRNA transcripts in both the brain and isolated cerebellar neurons indicates that insulin is in fact locally produced, although it does not exclude a role for exogenous insulin regulation of CNS functions.

The real-time quantitative RT-PCR studies demonstrated more abundant expression of insulin and IGF-I in cerebellar tissue compared with cultured cerebellar neurons, and higher levels of IGF-II mRNA in the isolated neurons compared with the tissue extracts. This suggests that insulin and IGF-I are predominantly expressed in cells other than granule neurons, whereas IGF-II is abundantly expressed in cerebellar granule neurons. The effects of ethanol on insulin gene expression were paralleled in the in vivo and in vitro systems, indicating that insulin gene expression, regardless of the source within the CNS, is impaired or inhibited by chronic gestational exposure to ethanol. In contrast, IGF-1 expression in both neurons and non-neuronal cells appears to be somewhat resistant to the toxic effects of ethanol. The apparently contradictory results observed with respect to IGF-II and IGF-II receptor expression in the brain and in cultured neuronal cells could be explained in part by an ethanol-induced shift in brain cell populations, i.e., ethanol exposure may result in increased proportions of IGF-II- and IGF-II receptor-positive non-neuronal cells in the brain. In both control and ethanol-exposed brains and in cultured neuronal cells, IGF-II mRNA transcripts were most abundant, followed by IGF-I, while insulin was expressed at four- or fivefold lower levels than IGF-I. This suggests that in the postnatal developing cerebellum, IGF-II has a broad role in mediating intracellular signaling related to growth and differentiation, whereas insulin and IGF-1 may have more specific and perhaps more tightly regulated functions at this stage of development (see below).

In previous studies, the roles of insulin and IGF-I signaling in relation to CNS growth, development, and function were divulged in part by the analysis of transgenic and knockout mouse models. Targeted gene mutation studies demonstrated that IGF-I and IGF-II stimulate prenatal brain growth, whereas only IGF-I stimulates postnatal brain growth [59]. During fetal development, insulin-stimulated signaling via its own receptor appears to be uncoupled and instead, the insulin receptor is activated by IGF-II [59]. Therefore, using the targeted mutation approach, IGF-II was demonstrated to be a bi-functional ligand capable of activating both insulin and IGF-I signaling mechanisms in the immature brain, although IGF-II is not as effective as insulin for mediating growth, energy metabolism, glucose homeostasis, survival, and cognition [59]. On the other hand, the findings of significantly reduced levels of insulin and increased levels of IGF-II gene expression, vis-à-vis cerebellar hypoplasia and impaired viability of cerebellar neurons in the ethanol-exposed group [38], highlight the importance of local insulin gene expression and further suggest that IGF-II, although strikingly up-regulated, cannot completely supplant the role of insulin-stimulated signaling in the developing brain.

The detection of IRS-1, IRS-2, and IRS-4 mRNA transcripts in cerebellar tissue indicates that each of these isoforms of IRS is expressed in the developing CNS. The analysis of IRS gene expression in isolated cerebellar neurons provided additional information about the molecules that mediate insulin and IGF signaling in neuronal cells during development. The similarly high levels of IRS-2 mRNA expression in cerebellar tissue and neurons indicate that this isoform of IRS is abundantly expressed in various cell types within the developing CNS. The similarly high levels of IRS-1 and IRS-2 in isolated neuronal cells suggest that developing neurons utilize signaling transmitted through each of these molecules. In contrast, the lower levels of IRS-4 in isolated neuronal cells compared with cerebellar tissue suggest that IRS-4 signaling

may be more important in non-neuronal cells in the developing cerebellum. These interpretations correspond with the previous observations that genetic depletion of IRS-1 results in retarded somatic growth with substantial reductions in the masses of skeletal muscle, heart, and liver, and relatively small reductions in brain weight [60], whereas genetic depletion of IRS-2 impairs neuronal proliferation and brain growth during development [61, 62], and genetic depletion of IRS-3 or IRS-4 produces no obvious phenotype [63]. IRS gene expression was not significantly different between the control and ethanol-exposed groups.

Since all of the results were normalized to 18S RNA transcripts, which were similarly abundant in the control and ethanol group samples, the differences noted above could not be attributed to global cell loss. Given the fact that chronic gestational exposure to ethanol results in significantly increased apoptosis in the brain, potential explanations for the severe muting of growth factor and growth factor receptor expression levels in the cultured neurons derived from ethanol-exposed pups include: (i) the phenotype of the population may have shifted due to selective loss of insulin/IGF-II-responsive neurons, and (ii) the corresponding genes may have been down-regulated in response to injury. In this regard, one of the more interesting findings was that the relative deficiencies in growth factor and growth factor receptor gene expression produced by gestational exposure to ethanol were worse in the cultured cells than in the brains. This suggests that considerable degrees of ethanol-mediated neurotoxicity leading to impaired insulin and IGF survival signaling occur in CNS neurons rather than non-neuronal elements.

Effects of ethanol on insulin and IGF-I RTK activities

Previous studies demonstrated ethanol inhibition of insulin receptor tyrosine phosphorylation, vis-à-vis intact insulin receptor protein expression [38]. That work was extended by measuring insulin and IGF-I RTK activities in cerebellar tissue and determining the degree to which ethanol impairs the functional activation of these receptors. RTK activity was measured in immunoprecipitates, and the levels were normalized to the insulin or IGF-I receptor protein levels detected by Western blot analysis of the corresponding immunoprecipitates. The studies demonstrated significantly reduced levels of insulin and IGF-I RTK activities in ethanol-exposed cerebella, indicating that signaling through both receptors is impaired by ethanol, despite adequate levels of receptor expression. These observations are consistent with previous in vitro experimental results obtained using neuronal cell lines and primary CNS neuronal cultures [11, 18, 38, 64, 65]. Ethanol inhibition of signaling through the insulin receptor would likely have a negative impact on energy metabolism and neuronal viability, whereas impaired signaling through the IGF-I receptor would likely have major inhibitory effects on brain growth [59]. The findings of reduced local growth factor production and impaired RTK activation are reminiscent of type 1 diabetes mellitus.

The mechanism by which ethanol inhibits insulin and IGF-I RTK activities was explored by investigating the potential role of increased phosphatase expression and phosphatase activity as negative regulators of signaling. Previous studies demonstrated that ethanol inhibition of insulin signaling downstream through PI3 kinase-Akt was mediated by increased expression and activation of PTEN phosphatase [38, 39]. PTP1b negatively regulates insulin sensitivity by dephosphorylating the insulin or IGF-I receptor. Since PTP1b is negatively regulated by Akt [66], which was inhibited by chronic gestational exposure to ethanol [38], further studies were conducted to determine if PTP1b expression and activity were increased in ethanol-exposed cerebellar tissue. Increased PTP1b expression and phosphatase activity could account for ethanol-associated reductions in insulin and IGF-I RTK activities. PTP-S/TCPTP is another negative regulator of insulin and IGF-I RTK, including in neural cells [55, 56], and we were interested to examine this with respect to the mRNA levels. PP1, which is ubiquitously expressed and regulates many functions, including glycogen metabolism and cell cycle progression [67], and PP2A, an inhibitor of src family kinases and therefore an inhibitor of growth [68, 69], were investigated because ethanol impairs both growth and survival in the developing CNS, and PP2A has an important role in negatively regulating the phosphorylation of neuronal cytoskeletal proteins, particularly tau [70] and neurofilament [71], which mediate the formation and stabilization of cell processes required for transport, connectivity, and plasticity.

The studies demonstrated significantly increased levels of PTP1b/TCPTP-PTP-S activity in ethanol-exposed relative to control cerebellar tissue, although there were no significant differences with respect to the mRNA levels of PTP1b, PTP-S, PP1, or PP2A. Since PTP1b and TCPTP are negative regulators of insulin and IGF-I RTKs, their increased activity could account for the constitutively reduced activation of insulin and IGF-I RTKs observed in the ethanol-exposed samples. The finding of increased PTP1b activity in ethanol-exposed brains is of further interest because in previous studies, we demonstrated that ethanol inhibition of insulin signaling downstream through PI3 kinase-Akt was mediated by increased activation of PTEN [38, 39], Together, these observations suggest that increased phosphatase activity may represent a general mechanism by which ethanol impairs insulin- and IGF-stimulated signaling in the developing brain.

Gestational exposure to ethanol inhibits glucose transporter gene expression, glucose transport, and ATP production

Potential consequences of impaired insulin and IGF-I signaling include inhibition of insulin-responsive gene expression and reduced cellular functions such as proliferation, neurite outgrowth, glucose utilization, phospholipid metabolism, and amino acid transport. In previous studies, we demonstrated significantly reduced levels of an important insulin-responsive gene, glyceraldehydes-3-phosphate dehydrogenase [72], in the ethanol-exposed cerebella [38], suggesting that CNS glucose utilization and energy metabolism were impaired by ethanol. In addition to regulating glucose utilization, insulin can stimulate glucose uptake. Glucose uptake is mediated by glucose transporter molecules termed GLUTs [73], and previous studies demonstrated that chronic gestational exposure to ethanol inhibits expression and function of GLUT molecules in the brain [74–76]. Correspondingly, the present work demonstrated significantly reduced levels of GLUT2 and GLUT4 gene expression, as well as reduced levels of ATP in cerebellar tissue from ethanol-exposed pups. Additional experiments conducted to determine if impairments in glucose uptake and ATP production represent early neurotoxic effects of ethanol revealed significantly reduced basal and insulin- or IGF-I-stimulated glucose uptake and ATP levels in cultured cerebellar granule neurons that had been exposed to ethanol for just 48 h. Therefore, ethanol-mediated abnormalities in neuronal energy balance occur following acute ethanol exposure and probably represent a very early lesion. Together, these observations link ethanol-impaired insulin signaling to deficiencies in uptake and utilization of glucose in the developing brain.

Acknowledgement. The author thank Ms. K. Cleveland for her assistance with glucose uptake assays. This work was supported by grants COBRE grant P20RR15578, AA02666, AA-02169, AA-11431, and AA12908 from the NIH.

1 Clarren S. K., Alvord E. J., Sumi S. M., Streissguth A. P. and Smith D. W. (1978) Brain malformations related to prenatal exposure to ethanol. J. Pediatr. **92:** 64–67
2 Maier S. E. and West J. R. (2001) Regional differences in cell loss associated with binge-like alcohol exposure during the first two trimesters equivalent in the rat. Alcohol **23:** 49–57
3 Minana R., Climent E., Barettino D., Segui J. M., Renau-Piqueras J. and Guerri C. (2000) Alcohol exposure alters the expression pattern of neural cell adhesion molecules during brain development. J. Neurochem. **75:** 954–964
4 Olney J. W., Ishimaru M. J., Bittigau P. and Ikonomidou C. (2000) Ethanol-induced apoptotic neurodegeneration in the developing brain. Apoptosis **5:** 515–521
5 Swanson D. J., King M. A. Walker D. W., and Heaton, M. B. (1995) Chronic prenatal ethanol exposure alters the normal ontogeny of choline acetyltransferase activity in the rat septohippocampal system. Alcohol Clin. Exp. Res. **19:** 1252–1260
6 Yanni P. A. and Lindsley T. A. (2000) Ethanol inhibits development of dendrites and synapses in rat hippocampal pyramidal neuron cultures. Brain Res. Dev. Brain Res. **120:** 233–243
7 Liesi P. (1997) Ethanol-exposed central neurons fail to migrate and undergo apoptosis. J. Neurosci. Res. **48:** 439–448
8 Ikonomidou C., Bittigau P., Ishimaru M. J., Wozniak D. F., Koch C., Genz K. et al. (2000) Ethanol-induced apoptotic neurodegeneration and fetal alcohol syndrome. Science **287:** 1056–1060
9 Zhang F. X., Rubin R. and Rooney T. A. (1998) Ethanol induces apoptosis in cerebellar granule neurons by inhibiting insulin-like growth factor 1 signaling. J. Neurochem. **71:** 196–204
10 de la Monte S. M., Neely T. R., Cannon J. and Wands J. R. (2001) Ethanol impairs insulin-stimulated mitochondrial function in cerebellar granule neurons. Cell. Mol. Life Sci. **58:** 1950–1960
11 de la Monte S. M. and Wands J. R. (2002) Chronic gestational exposure to ethanol impairs insulin-stimulated survival and mitochondrial function in cerebellar neurons. Cell. Mol. Life Sci. **59:** 882–893
12 Ramachandran V., Perez A., Chen J., Senthil D., Schenker S. and Henderson G. I. (2001) In utero ethanol exposure causes mitochondrial dysfunction, which can result in apoptotic cell death in fetal brain: a potential role for 4-hydroxynonenal. Alcohol Clin. Exp. Res. **25:** 862–871
13 de la Monte S. M. and Wands J. R. (2001) Mitochondrial DNA damage and impaired mitochondrial function contribute to apoptosis of insulin-stimulated ethanol-exposed neuronal cells. Alcohol Clin. Exp. Res. **25:** 898–906
14 Goodyer C. G., De S. L., Lai W. H., Guyda H. J. and Posner B. I. (1984) Characterization of insulin-like growth factor receptors in rat anterior pituitary, hypothalamus, and brain. Endocrinology **114:** 1187–1195
15 Gammeltoft S., Fehlmann M. and Van O. E. (1985) Insulin receptors in the mammalian central nervous system: binding characteristics and subunit structure. Biochimie **67:** 1147–1153
16 Hill J. M., Lesniak M. A., Pert C. B. and Roth J. (1986) Autoradiographic localization of insulin receptors in rat brain: prominence in olfactory and limbic areas. Neuroscience **17:** 1127–1138
17 de la Monte S. M., Ganju N., Banerjee K., Brown N. V., Luong T. and Wands J. R. (2000) Partial rescue of ethanol-induced neuronal apoptosis by growth factor activation of phosphoinositol-3-kinase. Alcohol Clin. Exp. Res. **24:** 716–726
18 Hallak H., Seiler A. E., Green J. S., Henderson A., Ross B. N. and Rubin R. (2001) Inhibition of insulin-like growth factor-I signaling by ethanol in neuronal cells. Alcohol Clin. Exp. Res. **25:** 1058–1064
19 Ullrich A., Bell J. R., Chen E. Y., Herrera R., Petruzzelli L. M., Dull T. J. et al. (1985) Human insulin receptor and its relationship to the tyrosine kinase family of oncogenes. Nature **313:** 756–761
20 O'Hare T. and Pilch P. F. (1990) Intrinsic kinase activity of the insulin receptor. Int. J. Biochem. **22:** 315–324
21 Myers M. G., Sun X. J. and White M. F. (1994) The IRS-1 signaling system. Trends Biochem. Sci. **19:** 289–293
22 Shpakov A. O. and Pertseva M. N. (2000) Structural and functional characterization of insulin receptor substrate proteins and the molecular mechanisms of their interaction with insulin superfamily tyrosine kinase receptors and effector proteins. Membr. Cell Biol. **13:** 455–484
23 Skolnik E. Y., Batzer A., Li N., Lee C. H., Lowenstein E., Mohammadi M. et al. (1993) The function of GRB2 in linking the insulin receptor to Ras signaling pathways. Science **260:** 1953–1955
24 Baltensperger K., Kozma L. M., Cherniack A. D., Klarlund J. K., Chawla A., Banerjee U. et al. (1993) Binding of the Ras activator son of sevenless to insulin receptor substrate-1 signaling complexes. Science **260:** 1950–1952

25 Sun X. J., Crimmins D. L., Myers M. J., Miralpeix M. and White M. F. (1993) Pleiotropic insulin signals are engaged by multisite phosphorylation of IRS-1. Mol. Cell Biol. **13:** 7418–7428

26 Lam K., Carpenter C. L., Ruderman N. B., Friel J. C. and Kelly K. L. (1994) The phosphatidylinositol 3-kinase serine kinase phosphorylates IRS-1: stimulation by insulin and inhibition by wortmannin. J. Biol. Chem. **269:** 20648–20652

27 Kandel E. S. and Hay N. (1999) The regulation and activities of the multifunctional serine/threonine kinase Akt/PKB. Exp. Cell Res. **253:** 210–229

28 Burgering B. M. and Coffer P. J. (1995) Protein kinase B (c-Akt) in phosphatidylinositol-3-OH kinase signal transduction. Nature **376:** 599–602

29 Pap M. and Cooper G. M. (1998) Role of glycogen synthase kinase-3 in the phosphatidylinositol 3-kinase/Akt cell survival pathway. J. Biol. Chem. **273:** 19929–19932

30 Weeren P. C. van, Bruyn K. M. de, Vries-Smits A. M. de, Lint J. van and Burgering B. M. (1998) Essential role for protein kinase B (PKB) in insulin-induced glycogen synthase kinase 3 inactivation: characterization of dominant-negative mutant of PKB. J. Biol. Chem. **273:** 13150–13156

31 Datta S. R., Dudek H., Tao X., Masters S., Fu H., Gotoh Y. et al. (1997) Akt phosphorylation of BAD couples survival signals to the cell-intrinsic death machinery. Cell **91:** 231–241

32 Hetman M., Cavanaugh J. E., Kimelman D. and Xia Z. (2000) Role of glycogen synthase kinase-3beta in neuronal apoptosis induced by trophic withdrawal. J. Neurosci. **20:** 2567–2574

33 Dudek H., Datta S. R., Franke T. F., Birnbaum M. J., Yao R., Cooper G. M. et al. (1997) Regulation of neuronal survival by the serine-threonine protein kinase Akt. Science **275:** 661–665

34 Eves E. M., Xiong W., Bellacosa A., Kennedy S. G., Tsichlis P. N., Rosner M. R. et al. (1998) Akt, a target of phosphatidylinositol 3-kinase, inhibits apoptosis in a differentiating neuronal cell line. Mol. Cell. Biol. **18:** 2143–2152

35 Condorelli F., Salomoni P., Cotteret S., Cesi V., Srinivasula S. M., Alnemri E. S. et al. (2001) Caspase cleavage enhances the apoptosis-inducing effects of BAD. Mol. Cell. Biol. **21:** 3025–3036.

36 Halestrap A. P., Doran E., Gillespie J. P. and O'Toole A. (2000) Mitochondria and cell death. Biochem. Soc. Trans. **28:** 170– 177

37 Hirsch T., Susin S. A., Marzo I., Marchetti P., Zamzami N. and Kroemer G. (1998) Mitochondrial permeability transition in apoptosis and necrosis. Cell Biol. Toxicol. **14:** 141–145

38 Xu J., Yeon J. E., Chang H., Tison G., Chen G. J., Wands J. and de la Monte S. M. (2003) Ethanol impairs insulin-stimulated neuronal survival in the developing brain: role of PTEN phosphatase. J. Biol. Chem. **278:** 26929–26937

39 Yeon J. E., Califano S., Xu J., Wands J. R. and Monte S. M. de la (2003) Potential role of PTEN phosphatase in ethanol-impaired survival signaling in the liver. Hepatology **38:** 703–714

40 Dahia P. L., Aguiar R. C., Alberta J., Kum J. B., Caron S., Sill H. et al. (1999) PTEN is inversely correlated with the cell survival factor Akt/PKB and is inactivated via multiple mechanisms in haematological malignancies. Hum. Mol. Genet. **8:** 185–193

41 Urso T., Gavaler J. S. and Van T. D. (1981) Blood ethanol levels in sober alcohol users seen in an emergency room. Life Sci. **28:** 1053–1056

42 Mohamed S. A., Nathaniel E. J., Nathaniel D. R. and Snell L. (1987) Altered Purkinje cell maturation in rats exposed prenatally to ethanol. I. Cytology. Exp. Neurol. **97:** 35–52

43 Ausubel F. M., Brent R., Kingston R. E., Moore D. D., Seidman J. G., Smith J. A. et al. (2002) Current Protocols in Molecular Biology, Wiley, New York

44 Banerjee K., Mohr L., Wands J. R. and Monte S. M. de la (1998) Ethanol inhibition of insulin signaling in hepatocellular carcinoma cells. Alcohol Clin. Exp. Res. **22:** 2093–2101

45 de la Monte S. M., Ganju N., Tanaka S., Banerjee K., Karl P. J., Brown N. V. et al. (1999) Differential effects of ethanol on insulin-signaling through the insulin receptor substrate-1. Alcohol Clin. Exp. Res. **23:** 770–777

46 Nikolic M., Dudek H., Kwon Y. T., Ramos Y. F. and Tsai L. H. (1996) The cdk5/p35 kinase is essential for neurite outgrowth during neuronal differentiation. Genes Dev. **10:** 816–825

47 Szabo A., Dalmau J., Manley G., Rosenfeld M., Wong E., Henson J. et al. (1991) HuD, a paraneoplastic encephalomyelitis antigen, contains RNA-binding domains and is homologous to Elav and Sex-lethal. Cell **67:** 325–333

48 Karl P. I. and Fisher S. E. (1993) Ethanol alters hormone production in cultured human placental trophoblasts. Alcohol Clin. Exp. Res. **17:** 816–821

49 Karl P. I. and Fisher S. E. (1994) Chronic ethanol exposure inhibits insulin and IGF-1 stimulated amino acid uptake in cultured human placental trophoblasts. Alcohol Clin. Exp. Res. **18:** 942–946

50 Dumke C. L., Wetter A. C., Arias E. B., Kahn C. R. and Cartee G. D. (2001) Absence of insulin receptor substrate-1 expression does not alter GLUT1 or GLUT4 abundance or contraction-stimulated glucose uptake by mouse skeletal muscle. Horm. Metab. Res. **33:** 696–700

51 Rasmussen S. K., Hansen L., Frevert E. U., Cohen P. T., Kahn B. B. and Pedersen O. (2000) Adenovirus-mediated expression of a naturally occurring Asp905Tyr variant of the glycogen-associated regulatory subunit of protein phosphatase-1 in L6 myotubes. Diabetologia **43:** 718–722

52 Moyers J. S., Bilan P. J., Reynet C. and Kahn C. R. (1996) Overexpression of Rad inhibits glucose uptake in cultured muscle and fat cells. J. Biol. Chem. **271:** 23111–23116

53 Silva A. M. da, Payao S. L., Borsatto B., Bertolucci P. H. and Smith M. A. (2000) Quantitative evaluation of the rRNA in Alzheimer's disease. Mech. Ageing Dev. **120:** 57–64

54 Payao S. L., Smith M. A., Winter L. M. and Bertolucci P. H. (1998) Ribosomal RNA in Alzheimer's disease and aging. Mech. Ageing Dev. **105:** 265–272

55 Klingler-Hoffmann M., Fodero-Tavoletti M. T., Mishima K., Narita Y., Cavenee W. K., Furnari F. B. et al. (2001) The protein tyrosine phosphatase TCPTP suppresses the tumorigenicity of glioblastoma cells expressing a mutant epidermal growth factor receptor. J. Biol. Chem. **276:** 46313–46318

56 Galic S., Klingler-Hoffmann M., Fodero-Tavoletti M. T., Puryer M. A., Meng T. C., Tonks N. K. et al. (2003) Regulation of insulin receptor signaling by the protein tyrosine phosphatase TCPTP. Mol. Cell. Biol. **23:** 2096–2108

57 Folli F., Ghidella S., Bonfanti L., Kahn C. R. and Merighi A. (1996) The early intracellular signaling pathway for the insulin/insulin-like growth factor receptor family in the mammalian central nervous system. Mol. Neurobiol. **13:** 155–183

58 D'Ercole A. J., Ye P., Calikoglu A. S. and Gutierrez-Ospina G. (1996) The role of the insulin-like growth factors in the central nervous system. Mol. Neurobiol. **13:** 227–255

59 Nakae J., Kido Y. and Accili D. (2001) Distinct and overlapping functions of insulin and IGF-I receptors. Endocr. Rev. **22:** 818–835

60 Pete G., Fuller C. R., Oldham J. M., Smith D. R., D'Ercole A. J., Kahn C. R. et al. (1999) Postnatal growth responses to insulin-like growth factor I in insulin receptor substrate-1-deficient mice. Endocrinology **140:** 5478–5487

61 Schubert M., Brazil D. P., Burks D. J., Kushner J. A., Ye J., Flint C. L. et al. (2003) Insulin receptor substrate-2 deficiency impairs brain growth and promotes tau phosphorylation. J. Neurosci. **23:** 7084–7092

62 Virkamaki A., Ueki K. and Kahn C. R. (1999) Protein-protein interaction in insulin signaling and the molecular mechanisms of insulin resistance. J. Clin. Invest. **103:** 931–943

63 Mauvais-Jarvis F., Kulkarni R. N. and Kahn C. R. (2002) Knockout models are useful tools to dissect the pathophysiology and genetics of insulin resistance. Clin. Endocrinol. **57:** 1–9

64 Seiler A. E., Ross B. N., Green J. S. and Rubin R. (2000) Differential effects of ethanol on insulin-like growth factor-I receptor signaling. Alcohol Clin. Exp. Res. **24:** 140–148
65 Seiler A. E., Ross B. N. and Rubin R. (2001) Inhibition of insulin-like growth factor-1 receptor and IRS-2 signaling by ethanol in SH-SY5Y neuroblastoma cells. J. Neurochem. **76:** 573–581
66 Ravichandran L. V., Chen H., Li Y. and Quon M. J. (2001) Phosphorylation of PTP1B at Ser(50) by Akt impairs its ability to dephosphorylate the insulin receptor. Mol. Endocrinol. **15:** 1768–1780
67 Ceulemans H. and Bollen M. (2004) Functional diversity of protein phosphatase-1, a cellular economizer and reset button. Physiol. Rev. **84:** 1–39
68 Nam J. S., Ino Y., Sakamoto M. and Hirohashi S. (2002) Src family kinase inhibitor PP2 restores the E-cadherin/catenin cell adhesion system in human cancer cells and reduces cancer metastasis. Clin. Cancer Res. **8:** 2430–2436
69 Yokoyama N. and Miller W. T. (2001) Inhibition of Src by direct interaction with protein phosphatase 2A. FEBS Lett. **505:** 460–464
70 Sontag E., Nunbhakdi-Craig V., Lee G., Bloom G. S. and Mumby M. C. (1996) Regulation of the phosphorylation state and microtubule-binding activity of Tau by protein phosphatase 2A. Neuron **17:** 1201–1207
71 Strack S., Westphal R. S., Colbran R. J., Ebner F. F. and Wadzinski B. E. (1997) Protein serine/threonine phosphatase 1 and 2A associate with and dephosphorylate neurofilaments. Brain Res. Mol. Brain Res. **49:** 15–28
72 Alexander B. M., Dugast I., Ercolani L., Kong X. F., Giere L. and Nasrin N. (1992) Multiple insulin-responsive elements regulate transcription of the GAPDH gene. Adv. Enzyme Regul. **32:** 149–159
73 Mueckler M. (1994) Facilitative glucose transporters. Eur. J. Biochem. **219:** 713–725
74 Handa R. K., DeJoseph M. R., Singh L. D., Hawkins R. A. and Singh S. P. (2000) Glucose transporters and glucose utilization in rat brain after acute ethanol administration. Metab. Brain Dis. **15:** 211–222
75 Hu I. C., Singh S. P. and Snyder A. K. (1995) Effects of ethanol on glucose transporter expression in cultured hippocampal neurons. Alcohol Clin. Exp. Res. **19:** 1398–1402
76 Singh S. P., Srivenugopal K. S., Yuan X. H., Jiang F. and Snyder A. K. (1993) Effects of ethanol ingestion on glucose transporter-1 protein and mRNA levels in rat brain. Life Sci. **53:** 1811–1819